Journal of the American College of Cardiology
© 2012 by the American College of Cardiology Foundation
Published by Elsevier Inc.

Vol. 59, No. 24, 2012
ISSN 0735-1097/$36.00
doi:10.1016/j.jacc.2012.01.060

Cyclic Adenosine Monophosphate Phosphodiesterase Type 4 Protects Against Atrial Arrhythmias

Cristina E. Molina, PhD,*† Jérôme Leroy, PhD,*† Wito Richter, PhD,‡ Moses Xie, BSc,‡ Colleen Scheitrum, BSc,‡ Illkyu-Oliver Lee, MD,§ Christoph Maack, MD,§ Catherine Rucker-Martin, PhD,†‖ Patrick Donzeau-Gouge, MD,¶ Ignacio Verde, PhD,# Anna Llach, PhD,** Leif Hove-Madsen, PhD,** Marco Conti, MD,‡ Grégoire Vandecasteele, PhD,*† Rodolphe Fischmeister, PhD*†

Châtenay-Malabry, Le Plessis Robinson, and Massy, France; San Francisco, California; Homburg/Saar, Germany; Covilhã, Portugal; and Barcelona, Spain

Objectives This study was designed to examine whether a cyclic adenosine monophosphate (cAMP) phosphodiesterase (PDE), PDE4, is expressed in human atrium and contributes to the control of electrical stability.

Background Atrial fibrillation is accompanied by a profound remodeling of membrane receptors and alterations in cAMP-dependent regulation of Ca^{2+} handling. Being responsible for cAMP hydrolysis, PDEs are likely to play a role in this setting. In the rodent heart, PDE4 contributes up to 60% of total cAMP-hydrolytic activity. However, its role in the human heart remains controversial.

Methods L-type Ca^{2+} current and spontaneous Ca^{2+} release were recorded in isolated human atrial myocytes. Intracellular cAMP was measured by live cell imaging using a fluorescence resonance energy transfer-based sensor. Contractile force and arrhythmias were recorded in human atrial trabeculae. PDE activity was measured in human atrial tissue from patients in sinus rhythm and permanent atrial fibrillation.

Results PDE4 is expressed in human atrial myocytes and accounts for approximately 15% of total PDE activity. PDE4D represents the major PDE4 subtype. PDE4 inhibition increased intracellular cAMP and L-type Ca^{2+} current and dramatically delayed their decay after a brief β-adrenergic stimulation. PDE4 inhibition also increased the frequency of spontaneous Ca^{2+} release at baseline, as well as the contractile response and the incidence of arrhythmias in human atrial strips during β-adrenergic stimulation. Total PDE activity decreased with age, and the relative PDE4 activity was lower in patients with permanent atrial fibrillation than in age-matched sinus rhythm controls.

Conclusions PDE4 is critical in controlling cAMP levels and thereby Ca^{2+} influx and release in human atrial muscle, hence limiting the susceptibility to arrhythmias. (J Am Coll Cardiol 2012;59:2182–90) © 2012 by the American College of Cardiology Foundation

Cyclic adenosine monophosphate (cAMP) elevation in human atrial myocytes (HAMs) leads to a positive chronotropic, inotropic, and lusitropic effect that is primarily mediated by protein kinase A (PKA)-dependent phosphorylation of key proteins, such as L-type Ca^{2+} channels (LTCCs), phospholamban, ryanodine receptor (RyR2), and troponin I (1). The most powerful and important mechanism that activates the cAMP pathway in HAMs is the

See page 2191

From *INSERM UMR-S 769, LabEx LERMIT, DHU-Torino, Châtenay-Malabry, France; †Université Paris-Sud, Châtenay-Malabry, France; ‡Department of Obstetrics, Gynecology, and Reproductive Sciences, Center for Reproductive Sciences, University of California–San Francisco, San Francisco, California; §Universität des Saarlandes, Klinik für Innere Medizin III, Homburg/Saar, Germany; ‖INSERM UMR-S 999, LabEx LERMIT, DHU-Torino, Hôpital Marie Lannelongue, Le Plessis Robinson, France; ¶Institut Hospitalier Jacques Cartier, Massy, France; #CICS-UBI, Centro de Investigação em Ciências da Saúde, Universidade da Beira Interior, Covilhã, Portugal; and the **Cardiovascular Research Centre, CSIC-ICCC and Cardiology Department, Hospital de la Santa Creu i Sant Pau, Barcelona, Spain.
This research was supported in part by the Fondation Leducq for the Transatlantic Network of Excellence cycAMP grant 06CVD02 to Drs. Fischmeister and Conti; European Union contract LSHM-CT-2005-018833/EUGeneHeart to Dr. Fischmeister; NIH grant HL092788 to Dr. Conti; the Fondation Lefoulon-Delalande to Dr. Molina; the Fondation de France and Agence Nationale de la Recherche grant 2010 BLAN 1139 01 to Dr. Vandecasteele; and by grants from the Spanish Ministry of Science and Technology CNIC2007-12 and SAF2007-60174 to Dr. Hove-Madsen. Dr. Maack is supported by the Deutsche Forschungsgemeinschaft (Emmy Noether Programm, KFO-196, and SFB894). All other authors have reported that they have no relationships relevant to the contents of this paper to disclose. Drs. Molina and Leroy contributed equally to this work.

Manuscript received May 18, 2011; revised manuscript received December 8, 2011, accepted January 9, 2012.

stimulation of β-adrenergic receptors (β-ARs) by norepinephrine released from the sympathetic nervous system in response to stress or exercise. β-ARs signal primarily through $G_{\alpha s}$-proteins, resulting in the stimulation of adenylyl cyclases and cAMP synthesis. β-AR signaling is rapidly terminated through several processes, among which cAMP degradation by cAMP phosphodiesterases (PDEs) plays a prominent role. PDEs comprise a large group of isoenzymes that are divided into 11 PDE families based on their substrate and inhibitor specificity and sequence homology (2). Of these, PDE3 and PDE4 contribute most of the cAMP-hydrolytic activity in rodent cardiomyocytes (3). Although the role of PDE3 in controlling contractile and electrical activity in human heart has been studied extensively (4,5), the role of PDE4 has not been investigated in detail.

The PDE4 family consists of 4 genes (*PDE4A*, *PDE4B*, *PDE4C*, and *PDE4D*), but only *PDE4A*, *PDE4B*, and *PDE4D* are expressed in the heart (6,7). Here, we demonstrate that all 3 isoforms are also expressed in isolated HAMs. We demonstrate that PDE4 contributes to cAMP hydrolysis in human atrium and thereby controls Ca^{2+} influx through LTCCs and thus contractility, both at basal and during β-AR stimulation. PDE4 inhibition in HAMs increases the frequency of nonpropagating Ca^{2+} release (Ca^{2+} sparks) and propagating Ca^{2+} release (Ca^{2+} waves), which is a source of spontaneous membrane depolarization and arrhythmias. Accordingly, PDE4 inhibition increased the incidence of arrhythmias during β-AR stimulation in human atrial tissue. Patients with permanent atrial fibrillation (AF) were found to have a decreased PDE4 activity as compared with patients in sinus rhythm. Thus, this study demonstrates that PDE4 controls cAMP- and PKA-dependent signaling in human atrium and protects against arrhythmias.

Methods

The study conformed to the principles outlined in the Declaration of Helsinki and was approved by the ethics committees of our institutions. All protocols for obtaining human cardiac tissue were approved by the ethics committees, and informed consent was obtained before cardiac surgery. Patient characteristics; drugs and methods used for isolation, culture, and infection of HAMs; L-type Ca^{2+} and transient inward current measurements; live cell imaging of intracellular cAMP; confocal Ca^{2+} imaging; preparation of protein extracts; PDE immunoprecipitation; immunocytochemistry; PDE activity assay; mechanoelectrical measurements; and data analysis and statistics are detailed in the supplemental methods section in the Online Appendix.

Results

Expression and localization of PDE4 in human right atrium. The 4 major cardiac cAMP PDEs expressed in rodent heart (3,6), PDE1, PDE2, PDE3, and PDE4, were also found to be expressed in human atrium (Fig. 1A). Of particular interest is the presence of PDE4, which accounts for approximately 15% of total cAMP-hydrolytic activity. Immunoprecipitation assays using PDE4 subtype selective antibodies revealed that the 3 cardiac PDE4 subtypes previously identified in rats (6), PDE4A, PDE4B, and PDE4D, are also expressed in human atrium, with PDE4D contributing the largest amount (Fig. 1B). PDE4C message is not found in expressed sequence tags (EST) databases of mouse, rat, and human heart, and the amount of PDE activity immunoprecipitated in preliminary experiments with anti-PDE4C antibodies was negligible compared with that of PDE4A, PDE4B, and PDE4D (data not shown). For these reasons, PDE4C was not investigated further. Western blot analysis revealed one major immunoreactive band for PDE4D in human atrium whose migration is consistent with that of PDE4D3, PDE4D8, or PDE4D9 (inset in Fig. 1B). Specific expression of PDE4 in HAMs also was demonstrated by immunostaining. PDE4 enzymes were detected at the Z-line of atrial myocytes, colocalized with the sarcomere-associated protein α-actinin (Fig. 1C).

Abbreviations and Acronyms

- **AF** = atrial fibrillation
- **β-AR** = β-adrenergic receptor
- **cAMP** = cyclic adenosine monophosphate
- **$[cAMP]_i$** = intracellular cyclic adenosine monophosphate
- **Ca^{2+} sparks** = nonpropagating Ca^{2+} release
- **Ca^{2+} waves** = propagating Ca^{2+} release
- **HAM** = human atrial myocyte
- **HF** = heart failure
- **$I_{Ca,L}$** = L-type Ca^{2+} channel current
- **Iso** = isoprenaline
- **LTCC** = L-type Ca^{2+} channel
- **PDE** = phosphodiesterase
- **PKA** = protein kinase A
- **Ro** = Ro 20-1724
- **RyR2** = ryanodine receptor
- **SR** = sinus rhythm

PDE4 controls basal intracellular cAMP concentration in HAMs. Intracellular cyclic adenosine monophosphate ($[cAMP]_i$) was measured in HAMs by live cell imaging using the fluorescence resonance energy transfer-based cAMP sensor Epac2-camps (8). Application of the β-AR agonist isoprenaline (Iso) (100 nM) during a 15-s pulse produced a rapid and transient change in the cyan fluorescent protein and yellow fluorescent protein fluorescence (Fig. 2A), leading to a transient increase of the cyan fluorescent protein-to-yellow fluorescent protein ratio (Fig. 2B), reflecting an increase in $[cAMP]_i$. Application of the PDE4 inhibitor Ro 20-1724 (Ro; 10 μM) produced a small but significant increase in basal $[cAMP]_i$ (Figs. 2C and 2E) that was approximately 50% smaller than that induced by cilostamide (1 μM), a PDE3 inhibitor (Figs. 2D and 2E). When the 2 PDEs were blocked simultaneously (Ro plus cilostamide), $[cAMP]_i$ increased further (Figs. 2C and 2D) to reach approximately 50% of the Iso response (Fig. 2E). These results indicate that PDE3 and PDE4 jointly control basal cAMP levels in HAMs.

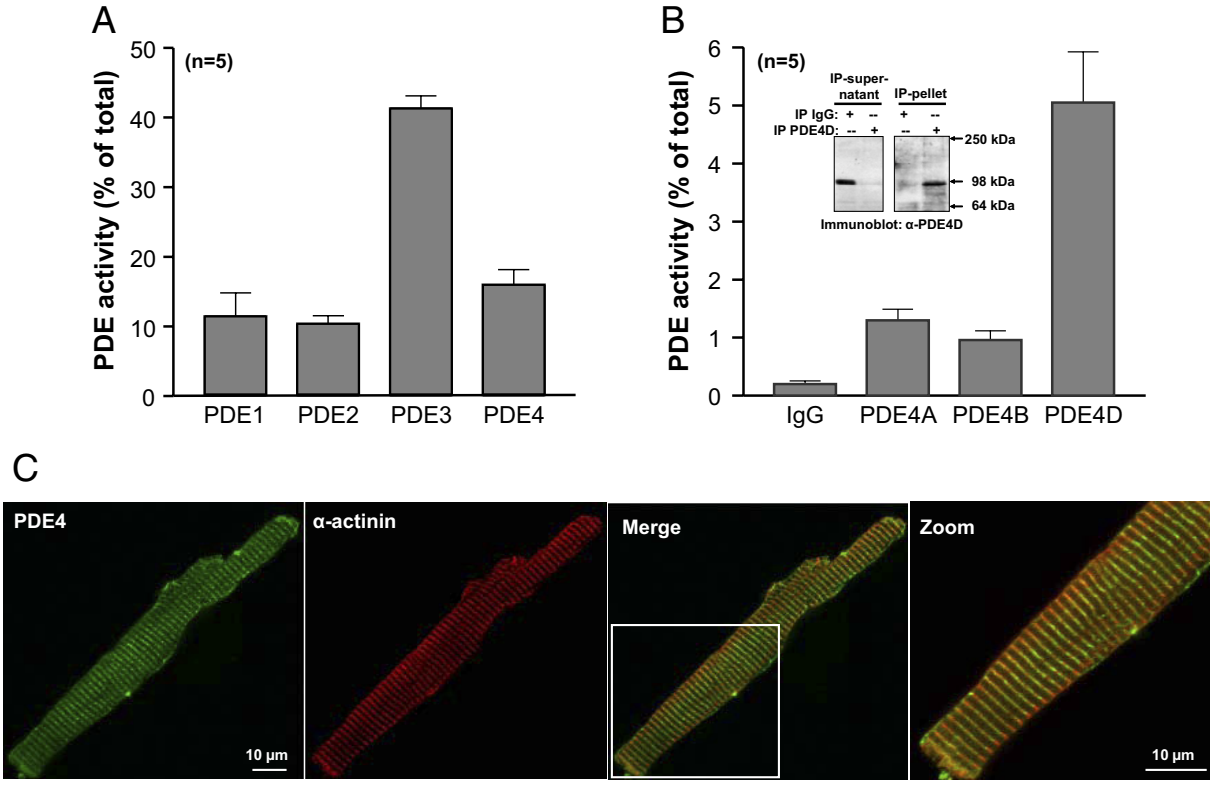

Figure 1 **Phosphodiesterase Families Expressed in Human Atrium**

(A) Detergent extracts prepared from human atrium were subjected to phosphodiesterase (PDE) activity assays in the absence or presence of PDE family-selective inhibitors using 1 μM cyclic adenosine monophosphate as substrate. Family-specific PDE activities were defined as the portion of total PDE activity inhibited by 20 μM vinpocetine (PDE1), 0.1 μM Bay60-7550 (PDE2), 10 μM cilostamide (PDE3), or 10 μM rolipram (PDE4). **(B)** PDE4 subtypes expressed in human atrium. Detergent extracts prepared from human atrium were subjected to immunoprecipitations (IP) using PDE4 subtype-selective antibodies. The amount of PDE activity recovered in the IP pellets corrected for the amount of protein used as IP input is reported. **(Inset)** sodium dodecyl sulfate polyacrylamide gel electrophoresis (SDS-PAGE) migration of PDE4 subtypes expressed in human atrium. Detergent extracts prepared from human atrium were subjected to coimmunoprecipitation assays using PDE4D-selective antibodies or normal immunoglobulin G (IgG) as a control. Shown is the PDE4D expression in cell extracts that had been depleted with either control IgG or PDE4D antibodies **(left)** and the PDE4D species recovered in the IP pellets **(right)** by Western blotting with PDE4D-selective antibodies. **(C)** Distribution of PDE4 in isolated human atrial myocytes. Isolated human atrial myocytes were stained with anti-PAN-PDE4 antibody (isoform nonspecific anti-PDE4 antibody) and with anti-α-actinin antibody. Superimposed images (merge) and magnification of the area within the white rectangle revealed an overlapping distribution of PDE4 with α-actinin.

PDE4 modulates cAMP and L-type Ca^{2+} current responses to β-AR stimulation in HAMs. To determine whether the control of basal $[cAMP]_i$ by PDE4 translates into biological functions, we examined whether PDE4 modulates the L-type Ca^{2+} current ($I_{Ca,L}$). As shown in Supplemental Figure 1A, Ro increased basal $I_{Ca,L}$ in a concentration-dependent manner and the effect was fully reversible. Next, we examined whether PDE4 controls the response of $I_{Ca,L}$ and $[cAMP]_i$ to Iso in HAMs. Figure 3 shows the average response of isolated HAMs to a brief β-AR stimulation with Iso (15 s, 100 nM). $[cAMP]_i$ (Fig. 3A) and $I_{Ca,L}$ (Fig. 3C) increased to reach a maximum at approximately 60 and 80 s, respectively, and then returned progressively to basal levels with a similar time course (Figs. 3B and 3D). Because the decay of the fluorescence ratio reflects hydrolysis of cAMP (9), the contribution of PDE4 to this process was examined by repeating the Iso application in the presence of Ro. PDE4 inhibition dramatically slowed down the decay phase of $[cAMP]_i$ (Fig. 3A) by increasing the time for half recovery by approximately 2-fold (Fig. 3B). The prolongation of the $[cAMP]_i$ response to Iso resulted in a similar 2-fold prolongation of the $I_{Ca,L}$ response (Figs. 3C and 3D) because of a prolonged PKA phosphorylation of LTCCs. Therefore, PDE4 plays a crucial role in controlling cAMP levels and $I_{Ca,L}$ on β-AR stimulation in HAMs. PDE3 contributes more than PDE4 to the recovery of the β-AR response, because cilostamide prolonged the decay phase of $[cAMP]_i$ and $I_{Ca,L}$ approximately 2.5-fold and 3-fold, respectively (Fig. 3).

PDE4 inhibition increases spontaneous Ca^{2+} release from the sarcoplasmic reticulum. Local Ca^{2+} sparks and Ca^{2+} waves were recorded in isolated HAMs. Continuous exposure of a HAM to 10 μM Ro for 15 min increased the frequency of Ca^{2+} sparks in a reversible manner (Fig. 4A). In HAMs with the membrane potential clamped at −80 mV, Ca^{2+} spark frequency was increased approximately

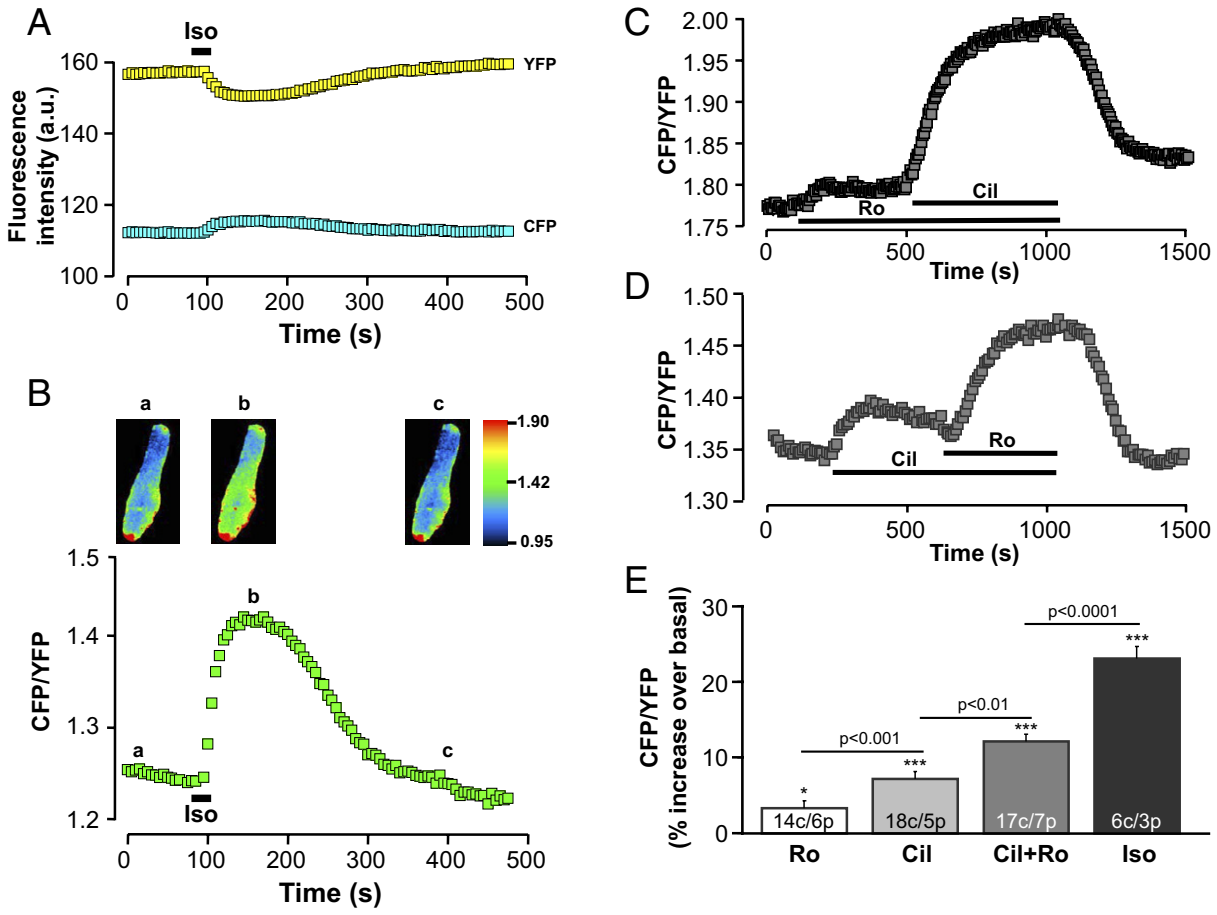

Figure 2 **Regulation of Basal Cyclic Adenosine Monophosphate Levels by PDE4 and PDE3 in Human Atrial Myocytes**

(A) Real-time measurement of cyclic adenosine monophosphate (cAMP) levels in response to β-adrenergic receptor (β-AR) stimulation. Human atrial myocytes (HAMs) were infected with the Epac2-camps adenovirus. The graph shows the time course of cyan fluorescent protein (CFP) and yellow fluorescent protein (YFP) emissions in response to a brief application of isoprenaline (Iso; 100 nM, 15 seconds). Transient cAMP binding to the sensor induces a transient decrease in fluorescence resonance energy transfer between CFP (excited at 440 ± 20 nm) and YFP visualized by a simultaneous increase in donor emission (CFP; **blue squares**) and a decrease in acceptor emission (YFP; **yellow squares**). Acquisitions were performed every 5 seconds. **(B)** Time course of the corrected CFP-to-YFP ratio. The pseudocolor images on top were obtained at the times indicated by the corresponding letters in the bottom graph. **(C)** Representative experiment showing the time course of the cAMP signal elicited in control, Ro 20-1724 (Ro; 10 μM), Ro plus cilostamide (Cil; 1 μM), and washout. **(D)** Representative experiment showing the time course of the cAMP signal elicited in control, Cil, Cil plus Ro, and washout. **(E)** Summary of the effects of Ro, Cil, Cil plus Ro, and Iso on cAMP levels expressed as percentage of increase of CFP-to-YFP ratio over its control value. The bar graphs are the mean ± SEM of the number of cells (c) and patients (p) indicated. *$p < 0.05$ versus control; ***$p < 0.001$ versus control. Abbreviations as in Figure 1.

3-fold by PDE4 inhibition (Fig. 4B), whereas neither Ca^{2+} spark amplitude nor the time constant for decay were modified (data not shown). Ro also increased the frequency of spontaneous Ca^{2+} waves and inward Na^{+}/Ca^{2+}-exchange current (Fig. 4C). On average, PDE4 inhibition increased the spontaneous Ca^{2+} wave frequency approximately 3-fold at −80 mV (Fig. 4D), but the effect was not significant when the holding potential was increased to −50 mV, possibly because the wave frequency already was near maximum in the absence of Ro. These results indicate that PDE4 activity is necessary to prevent spontaneous Ca^{2+} release from the sarcoplasmic reticulum, which is a source of spontaneous membrane depolarization and arrhythmias.

PDE4 inhibition increases frequency of arrhythmias during β-AR stimulation. Mechanoelectrical measurements were performed on human trabeculae isolated from the right atrium of 9 patients. PDE4 inhibition with 10 μM Ro had no effect on the force of contraction under basal conditions (Online Fig. 2A). However, Ro increased the positive inotropic effect of cilostamide (Online Figs. 2A and 2B) or of a submaximal β-AR stimulation of 10 nM Iso (Online Figs. 2C and 2D). Interestingly, arrhythmias occurred in the combined presence of PDE inhibitors and Iso in several of these experiments. Additional mechanoelectrical measurements thus were performed to test systematically whether PDE4 inhibition may promote arrhythmias. Furthermore, we addressed which β-AR subtype may be

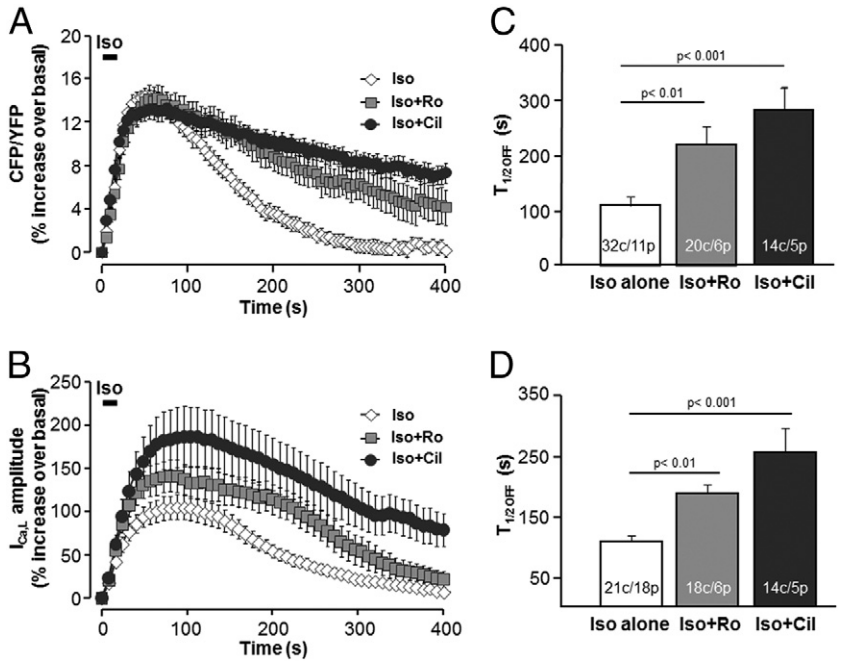

Figure 3 **PDE Regulation of the β-AR Response**

Average time course of the changes of **(A)** CFP-to-YFP ratio and **(B)** $I_{Ca,L}$ amplitude during a brief β-AR stimulation with Iso (100 nM, 15 seconds) alone or when Ro (10 μM) or Cil (1 μM) were added to the Iso solution and in the washout solution to inhibit PDE4 and PDE3, respectively. Mean values of the time for 50% recovery ($T_{1/2\,OFF}$) of the **(C)** fluorescence resonance energy transfer ratio and **(D)** $I_{Ca,L}$ amplitude. The **symbols** and **bar graphs** indicate the mean ± SEM of the number of cells (c) and patients (p). Other abbreviations as in Figures 1 and 2.

responsible for potential proarrhythmic effects of PDE inhibition. Selective β_1-AR stimulation with increasing concentrations of norepinephrine in the presence of a β_2-AR antagonist (ICI 118.551, 50 nM) increased the force of contraction (Fig. 5A), and spontaneous, nontriggered contractions were observed in less than 20% of fibers for norepinephrine concentrations of more than 3 μM (Fig. 5C). However, when PDE4 was blocked by rolipram (100 nM), these spontaneous contractions were observed at lower norepinephrine concentrations and were approximately 2-fold more frequent (40%) at higher concentrations (Figs. 5B and 5C). PDE3 inhibition with milrinone (1 μM) had a comparable effect (Fig. 5C). In contrast, no spontaneous contractions were observed on β_2-AR stimulation with epinephrine in the presence of the β_1-AR antagonist CGP207.12A (300 nM), even during PDE3 inhibition (Fig. 5D). However, inhibition of PDE4 had a dramatic effect, causing spontaneous contractions to occur in up to 40% of the trabeculae at the highest epinephrine concentrations (Fig. 5D).

AF is linked to a decrease in PDE4 activity. Because PDE4 seems to be critical in controlling $[cAMP]_i$, $I_{Ca,L}$, sarcoplasmic reticulum Ca^{2+} release, and contraction in the human atrium and its inhibition leads to atrial arrhythmias, we tested whether a change in PDE4 activity might take place during AF. Total PDE and PDE4 activity was measured in right atrial tissues from 18 patients in sinus rhythm (SR) and 7 patients with permanent AF. Eleven patients with heart failure (HF) were also included in this study because HF patients are at substantially increased risk of having AF (10). Mean values for total PDE were smaller in patients with HF and AF than those in SR (Fig. 6A), but the difference (approximately a 25% decrease) approached statistical significance ($p = 0.059$) only when comparing SR and AF patients. More importantly, PDE4 activity decreased by almost 50% ($p = 0.029$) in AF (17.1 ± 3.9 pmol/min per mg) as compared with SR patients (32.9 ± 3.9 pmol/min per mg). Although the age of the patients was not significantly different in the 3 groups ($p = 0.071$ for AF vs. SR; $p = 0.136$ for HF vs. SR), patients in the SR group were on average younger (66.8 ± 3.0 years) than in the HF group (73.2 ± 2.0 years) or AF group (76.4 ± 2.3 years). This raised the possibility that the changes in PDE activities might be the result of aging, rather than of the cardiac disease. Indeed, when total PDE activity for SR patients was plotted against patient age, a linear regression analysis showed a significant reduction with age ($p = 0.0054$) (Fig. 6B). Thus, to match the average age of the HF and AF groups, only the SR patients who were 59 years of age or older (mean age: 72.0 ± 2.2 years, $n = 14$) were included in subsequent analysis. The contribution of PDE4 to total PDE activity was found to be reduced in HF and AF patients as compared with this SR group, but the difference (approximately a 25% decrease) approached statistical significance ($p = 0.057$) only when comparing

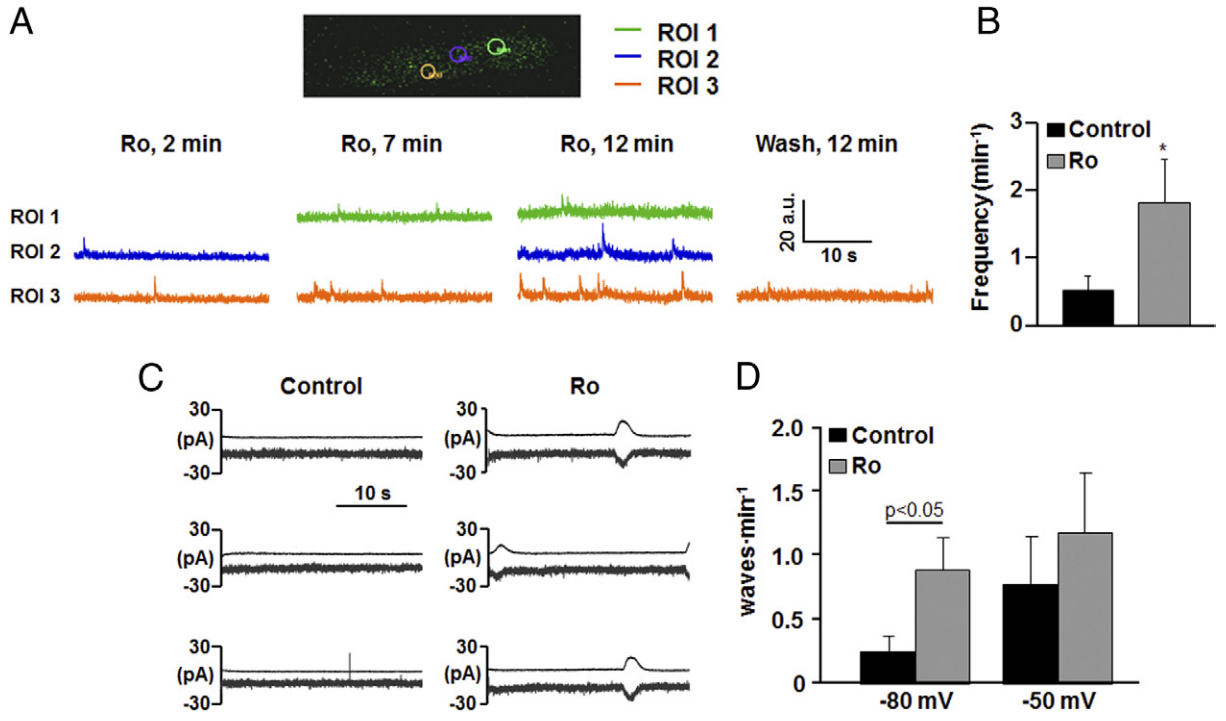

Figure 4 PDE4 Inhibition Increases Spontaneous Sarcoplasmic Reticulum Ca^{2+} Release

(A) Confocal image of a human atrial myocyte with 3 regions of interest (ROIs) where nonpropagating Ca^{2+} release (Ca^{2+} sparks) and propagating Ca^{2+} release (Ca^{2+} waves) were detected 2, 7, and 12 min after exposure to 10 μM Ro and 12 min after washout. No sparks were detected before exposure to Ro or after 17 min of wash. **(B)** Average effect (mean ± SEM) of Ro on the spark frequency at −80 mV in 15 myocytes from 10 patients. *$p < 0.05$ versus control. **(C)** Simultaneous recordings of the global Ca^{2+} signal **(upper trace)** and the whole membrane current **(lower trace)**. The figure shows consecutive traces of 28 s duration recorded before (control) or 10 to 12 min after exposure of the myocyte to 10 μM Ro. The Ca^{2+} signal is in a.u. **(D)** Average effect (mean ± SEM) of Ro on the spontaneous Ca^{2+} wave frequency in 16 myocytes from 11 patients clamped at −80 or −50 mV. Other abbreviations as in Figures 1 and 2.

age-matched SR and AF patients (Fig. 6C). These findings support the hypothesis that a decrease in PDE4 activity may be associated with the development of AF.

Discussion

Our study demonstrates that PDE4 is expressed in human atrium as well as in isolated HAMs, with PDE4D being the major isoform. Despite the fact that its activity is rather modest (approximately 15% of total PDE activity), PDE4 is central in controlling $[cAMP]_i$, Ca^{2+} influx through LTCCs, spontaneous Ca^{2+} release from the sarcoplasmic reticulum, and contractility. PDE4 seems particularly important in regulating the β-AR response of human atrial muscle, because inhibition of PDE4 leads to an increase in the positive inotropic effect of a β-AR stimulation and to a dramatic prolongation of the rise in $[cAMP]_i$ and $I_{Ca,L}$ amplitude. PDE4 inhibition also increased the propensity of atrial arrhythmias during either β_1-AR or β_2-AR stimulation. Because the relative contribution of PDE4 to the total cAMP hydrolytic activity decreased in patients with permanent AF, we propose that PDE4 serves a protective role against arrhythmias in human atrial muscle.

The PDE4 family is encoded by 4 genes (*PDE4A*, *PDE4B*, *PDE4C*, and *PDE4D*), but only *PDE4A*, *PDE4B*, and *PDE4D* are expressed in cardiac tissue (6,7). So far, most of our knowledge in heart tissue concerns the *PDE4D* gene (11), and long variants of this gene expressed in heart include the isoforms PDE4D3, PDE4D5, PDE4D8, and PDE4D9 (12). PDE4D5, PDE4D8, and PDE4D9 were shown to interact differentially with β_1-AR and β_2-AR subtypes in neonatal cardiac myocytes, either directly or by binding to β-arrestin (13–15). PDE4D3 was found in macromolecular signaling complexes regulating 2 major players of excitation-contraction coupling in rodent heart: the slow delayed rectifier K^+ current (16) and the ryanodine receptor RyR2 (17). Interestingly, inhibition of PDE4D leads to an increased PKA activation of the slow delayed rectifier K^+ current (16), which can contribute to AF (18). Here we found that PDE4D was the dominant member of the PDE4 family expressed in human atrium. Pharmacological inhibition of PDE4 (which includes inhibition of PDE4D) increased Ca^{2+} spark frequency in HAMs and led to the initiation and propagation of Ca^{2+} waves (Fig. 4). These Ca^{2+} waves in turn generated a transient inward Na^+/Ca^{2+}-exchange current as a result of elimination of

JACC Vol. 59, No. 24, 2012
June 12, 2012:2182–90

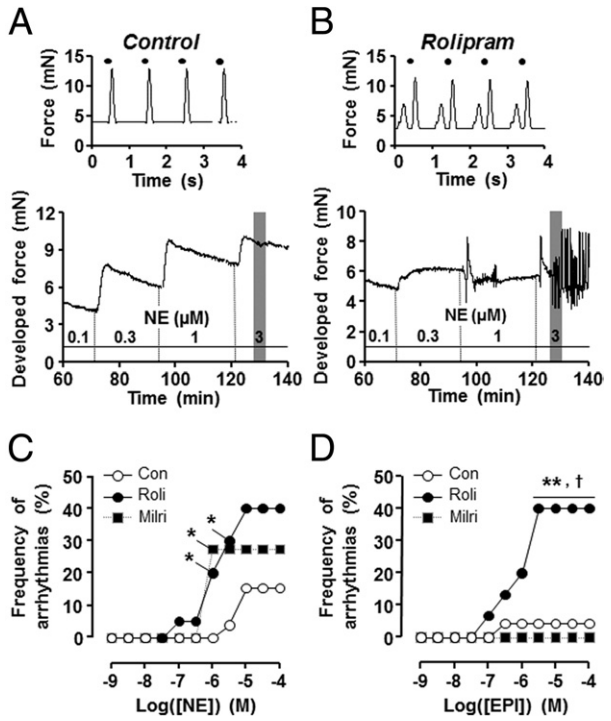

Figure 5 **PDE4 Inhibition Increases Frequency of Arrhythmias After β_1-AR and β_2-AR Stimulation in Human Atrial Myocardium**

Human atrial muscle strip preparations were stimulated at 1 Hz and were exposed to cumulative concentrations of norepinephrine (NE) in the presence of ICI 118.551 (50 nM) or epinephrine (EPI) in the presence of CGP207.12A (300 nM) to stimulate selectively β_1-AR or β_2-ARs, respectively. Experiments were carried out in the absence (control) or presence of rolipram (Roli; 100 nM) or milrinone (Milri; 1 μM). Representative traces of NE in **(A)** the absence and **(B)** the presence of rolipram, respectively. The **top traces** indicate original contractions recorded during the **gray shaded areas** in the **bottom graphs**. **Black dots** indicate the time points of electrical stimulation. Cumulative frequency of arrhythmias **(C)** after β_1-AR and **(D)** β_2-AR stimulation in the absence (Con; n = 26 for β_1-AR and n = 23 for β_2-AR stimulation) and presence of rolipram (Roli; n = 20/15) or Milrinone (Milri; n = 11/11), respectively. *p < 0.05 and **p <0.01 versus control and †p < 0.05 versus milrinone (Fisher exact test, respectively). Abbreviations as in Figure 2.

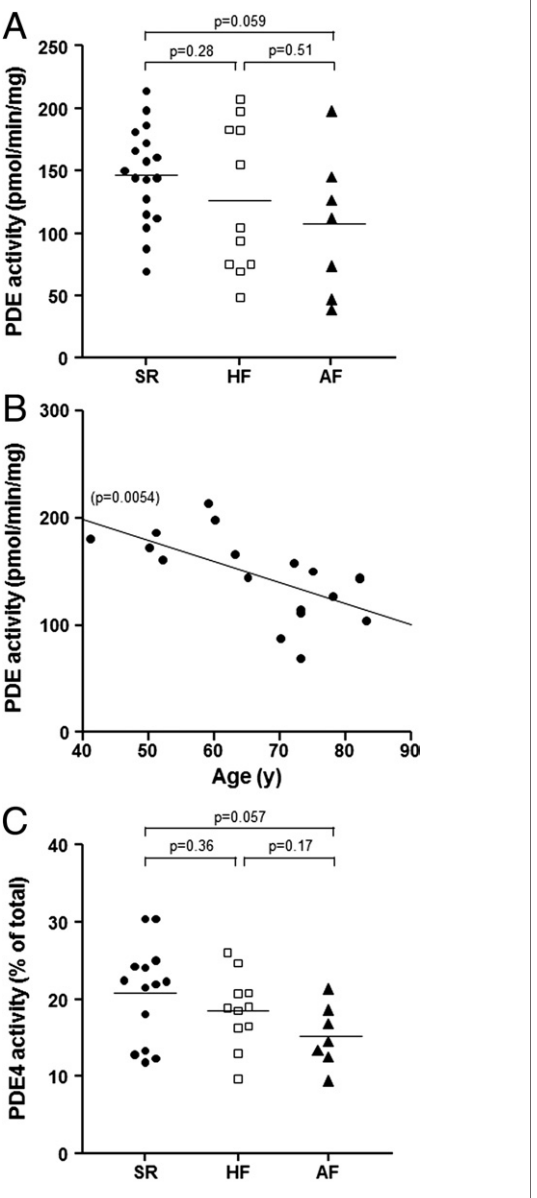

Figure 6 **Measurements of Total PDE and PDE4 Activity in Human Atrial Tissues**

(A) Individual and mean values for total PDE activity measured in right atrial tissues obtained from patients with sinus rhythm (SR), heart failure (HF; i.e., patients with ejection fraction < 60%), or permanent atrial fibrillation (AF). **(B)** Plot of the total PDE activity as a function of the patient's age. A linear regression analysis is shown. **(C)** PDE4 activity relative to total in age-matched patients in the 3 groups: SR, HF, and AF. For statistical evaluation, an unpaired Student *t* test was used in **(A)** and **(C)**, and an F test was used in **(B)** to tests if the slope was significantly different from 0. Abbreviations as in Figure 1.

cytosolic Ca^{2+} via the Na^+/Ca^{2+} exchanger (Fig. 4), which can give rise to delayed after-depolarizations (19). Importantly, Ca^{2+} spark frequency is also increased in HAMs from AF patients (20–22), coinciding with an increased phosphorylation of the RyR2 at Ser^{2808} in right atrial samples from patients with AF (21–23), and an increased open probability of RyR2 resulting from PKA hyperphosphorylation has been reported in an AF animal model (23). Moreover, mice deficient in the *PDE4D* gene have an increased sensitivity to exercise-induced ventricular arrhythmias resulting from PKA hyperphosphorylation of RyR2 and abnormal Ca^{2+} release as a result of calstabin dissociation from the channel (17). Thus, there is strong evidence to suggest that PDE4 inhibition may lead to abnormal Ca^{2+} release in human atrial cardiomyocytes via RyR2 hyperphosphorylation. Accordingly, PDE4 inhibition in human atrial trabeculae increased the incidence of arrhythmias during β-AR stimulation (Fig. 5).

PDE4 inhibition increased both basal $I_{Ca,L}$ (Online Fig. 1) and spontaneous Ca^{2+} sparks (Fig. 4) in HAMs. Yet, live cell imaging showed a limited increase in basal $[cAMP]_i$ on PDE4 inhibition (Fig. 2). By comparison, the increase in

$[cAMP]_i$ was twice as large when PDE3 was inhibited and 4 times larger when both PDE3 and PDE4 were blocked simultaneously. Thus, PDE4 inhibition alone may lead to cAMP rise in microdomains close to the LTCCs and the RyR2 that are either too small or not readily accessible to the cAMP probe.

Although our study demonstrates that an acute inhibition of PDE4 increases the activity of LTCCs, the observed decrease in PDE4 activity in AF patients is not accompanied by a commensurate increase in $I_{Ca,L}$ amplitude in HAMs from AF patients. On the contrary, reductions in $I_{Ca,L}$ have been observed consistently in atrial myocytes from patients with permanent AF (24,25) or from patients in SR with a high risk of AF (26) (for a review, see ref 27). A possible explanation for this is that stimulation of $I_{Ca,L}$ by PDE4 inhibition is the result of PKA phosphorylation of functional LTCCs, whereas it is generally agreed (25) that the reduction of $I_{Ca,L}$ in AF is the result of downregulation of the messenger ribonucleic acid encoding the Cav1.2 α-subunit, causing a reduction in the number of functional channels (27).

Clinical implications. The incidence and prevalence of AF increases progressively with age, and approximately 50% of patients with AF are 75 years of age or older (28). Advanced age is also a potent risk factor for stroke in patients with AF, and the proportion of strokes attributable to AF increases exponentially with age (28). Interestingly, an association between PDE4D and cardioembolic stroke was reported by the investigators of the Icelandic deCODE study (deCODE Genetics, Reykjavik, Iceland) (29). Although the so-called causative mutation has not been identified, single nucleotide polymorphisms in the *PDE4D* region are associated with ischemic stroke in many different populations (30). Although none of the single nucleotide polymorphisms identified affects the catalytic site of the enzyme, they are associated with a reduced messenger ribonucleic acid level for different PDE4D isoforms (29). Yet, to our surprise, none of the genetic studies published have considered the atrium as a possible target for the observed reduction in PDE4D expression. Because a rise in cAMP in vascular and inflammatory cells or in platelets would lead to vasorelaxation or would inhibit cell growth, proliferation, migration, neointima formation, inflammation, and platelet aggregation, it is unlikely that a reduction in PDE4D expression in one of these cell types would increase the risk for cardioembolic stroke. Here, we demonstrate that PDE4D is the major PDE4 isoform expressed in HAMs. Hence, our study suggests a possible link between PDE4D and cardiogenic stroke that involves abnormal intracellular Ca^{2+} handling in atrial myocytes that predisposes individuals to AF.

Acknowledgments

The authors thank Patrick Lechêne and Florence Lefebvre for their skillful technical assistance; Valérie Nicolas, Imaging Core Facility, IFR141-IPSIT, Faculty of Pharmacy, University Paris-Sud, for technical assistance with confocal microscopy; the Department of Cardiology and Cardiac Surgery at Hospital de Sant Pau for providing human atrial tissue samples; and Dr. Montserrat Barriga for invaluable help with the Ca^{2+} spark analysis.

Reprints requests and correspondence: Dr. Rodolphe Fischmeister, INSERM UMR-S 769, Faculté de Pharmacie, Université Paris-Sud, F-92296 Châtenay-Malabry, France. E-mail: rodolphe.fischmeister@inserm.fr.

REFERENCES

1. Bers DM. Cardiac excitation-contraction coupling. Nature 2002;415:198–205.
2. Conti M, Beavo JA. Biochemistry and physiology of cyclic nucleotide phosphodiesterases: essential components in cyclic nucleotide signaling. Ann Rev Biochem 2007;76:481–511.
3. Rochais F, Abi-Gerges A, Horner K, et al. A specific pattern of phosphodiesterases controls the cAMP signals generated by different G_s-coupled receptors in adult rat ventricular myocytes. Circ Res 2006;98:1081–8.
4. Packer M, Carver JR, Rodeheffer RJ, et al. Effect of oral milrinone on mortality in severe chronic heart failure. The PROMISE Study Research Group. N Engl J Med 1991;325:1468–75.
5. Christ T, Engel A, Ravens U, Kaumann AJ. Cilostamide potentiates more the positive inotropic effects of (−)-adrenaline through β_2-adrenoceptors than the effects of (−)-noradrenaline through β_1-adrenoceptors in human atrial myocardium. Naunyn Schmiedebergs Arch Pharmacol 2006;374:249–53.
6. Kostic MM, Erdogan S, Rena G, et al. Altered expression of PDE1 and PDE4 cyclic nucleotide phosphodiesterase isoforms in 7-oxo-prostacyclin-preconditioned rat heart. J Mol Cell Cardiol 1997;29:3135–46.
7. Richter W, Xie M, Scheitrum C, et al. Conserved expression and functions of PDE4 in rodent and human heart. Basic Res Cardiol 2011;106:249–62.
8. Nikolaev VO, Bunemann M, Hein L, Hannawacker A, Lohse MJ. Novel single chain cAMP sensors for receptor-induced signal propagation. J Biol Chem 2004;279:37215–8.
9. Leroy J, Abi-Gerges A, Nikolaev VO, et al. Spatiotemporal dynamics of β-adrenergic cAMP signals and L-type Ca^{2+} channel regulation in adult rat ventricular myocytes: role of phosphodiesterases. Circ Res 2008;102:1091–100.
10. Heist EK, Ruskin JN. Atrial fibrillation and congestive heart failure: risk factors, mechanisms, and treatment. Prog Cardiovasc Dis 2006;48:256–69.
11. Houslay MD, Baillie GS, Maurice DH. cAMP-Specific phosphodiesterase-4 enzymes in the cardiovascular system: a molecular toolbox for generating compartmentalized cAMP signaling. Circ Res 2007;100:950–66.
12. Richter W, Jin SL, Conti M. Splice variants of the cyclic nucleotide phosphodiesterase PDE4D are differentially expressed and regulated in rat tissue. Biochem J 2005;388:803–11.
13. Baillie GS, Sood A, McPhee I, et al. β-Arrestin-mediated PDE4 cAMP phosphodiesterase recruitment regulates β-adrenoceptor switching from G_s to G_i. Proc Natl Acad Sci U S A 2003;100:941–5.
14. Richter W, Day P, Agraval R, et al. Signaling from β_1- and β_2-adrenergic receptors is defined by differential interactions with PDE4. Embo J 2008;27:384–93.
15. De Arcangelis V, Liu R, Soto D, Xiang Y. Differential association of phosphodiesterase 4D isoforms with β_2-adrenoceptor in cardiac myocytes. J Biol Chem 2009;284:33824–32.
16. Terrenoire C, Houslay MD, Baillie GS, Kass RS. The cardiac I_{Ks} potassium channel macromolecular complex includes the phosphodiesterase PDE4D3. J Biol Chem 2009;284:9140–6.
17. Lehnart SE, Wehrens XHT, Reiken S, et al. Phosphodiesterase 4D deficiency in the ryanodine receptor complex promotes heart failure and arrhythmias. Cell 2005;123:23–35.

18. Sampson KJ, Terrenoire C, Cervantes DO, et al. Adrenergic regulation of a key cardiac potassium channel can contribute to atrial fibrillation: evidence from an I_{Ks} transgenic mouse. J Physiol 2008;586:627–37.
19. Cheng H, Lederer WJ. Calcium sparks. Physiol Rev 2008;88:1491–545.
20. Hove-Madsen L, Llach A, Bayes-Genis A, et al. Atrial fibrillation is associated with increased spontaneous calcium release from the sarcoplasmic reticulum in human atrial myocytes. Circulation 2004;110:1358–63.
21. Llach A, Molina CE, Prat-Vidal C, et al. Abnormal calcium handling in atrial fibrillation is linked to up-regulation of adenosine A2A receptors. Eur Heart J 2011;32:721–9.
22. Neef S, Dybkova N, Sossalla S, et al. CaMKII-dependent diastolic SR Ca^{2+} leak and elevated diastolic Ca^{2+} levels in right atrial myocardium of patients with atrial fibrillation. Circ Res 2010;106:1134–44.
23. Vest JA, Wehrens XH, Reiken SR, et al. Defective cardiac ryanodine receptor regulation during atrial fibrillation. Circulation 2005;111:2025–32.
24. Le Grand B, Hatem S, Deroubaix E, Couetil J, Coraboeuf E. Depressed transient outward and calcium currents in dilated human atria. Cardiovasc Res 1994;28:548–56.
25. Christ T, Boknik P, Wohrl S, et al. L-type Ca^{2+} current downregulation in chronic human atrial fibrillation is associated with increased activity of protein phosphatases. Circulation 2004;110:2651–7.
26. Dinanian S, Boixel C, Juin C, et al. Downregulation of the calcium current in human right atrial myocytes from patients in sinus rhythm but with a high risk of atrial fibrillation. Eur Heart J 2008;29:1190–7.
27. Nattel S, Maguy A, Le Bouter S, Yeh YH. Arrhythmogenic ion-channel remodeling in the heart: heart failure, myocardial infarction, and atrial fibrillation. Physiol Rev 2007;87:425–56.
28. Rich MW. Epidemiology of atrial fibrillation. J Interv Card Electrophysiol 2009;25:3–8.
29. Gretarsdottir S, Thorleifsson G, Reynisdottir ST, et al. The gene encoding phosphodiesterase 4D confers risk of ischemic stroke. Nat Genetics 2003;35:131–8.
30. Munshi A, Kaul S. Stroke genetics—focus on PDE4D gene. Int J Stroke 2008;3:188–92.

Key Words: arrhythmia ■ atrial fibrillation ■ PDE4 ■ phosphodiesterase.

APPENDIX

For a supplemental Methods section, please see the online version of this article.